Suppression of hippocampal TRPM7 protein prevents delayed neuronal death in brain ischemia

Hong-Shuo Sun[1], Michael F Jackson[2,3], Loren J Martin[4], Karen Jansen[5], Lucy Teves[1], Hong Cui[1], Shigeki Kiyonaka[6], Yasuo Mori[6], Michael Jones[1], Joan P Forder[1], Todd E Golde[5], Beverley A Orser[2,4,7], John F MacDonald[2,3] & Michael Tymianski[1,2,4,8]

Cardiac arrest victims may experience transient brain hypoperfusion leading to delayed death of hippocampal CA1 neurons and cognitive impairment. We prevented this in adult rats by inhibiting the expression of transient receptor potential melastatin 7 (TRPM7), a transient receptor potential channel that is essential for embryonic development, is necessary for cell survival and trace ion homeostasis *in vitro*, and whose global deletion in mice is lethal. TRPM7 was suppressed in CA1 neurons by intrahippocampal injections of viral vectors bearing shRNA specific for TRPM7. This had no ill effect on animal survival, neuronal and dendritic morphology, neuronal excitability, or synaptic plasticity, as exemplified by robust long-term potentiation (LTP). However, TRPM7 suppression made neurons resistant to ischemic death after brain ischemia and preserved neuronal morphology and function. Also, it prevented ischemia-induced deficits in LTP and preserved performance in fear-associated and spatial-navigational memory tasks. Thus, regional suppression of TRPM7 is feasible, well tolerated and inhibits delayed neuronal death *in vivo*.

Hypoxic-ischemic injuries to the mammalian brain elicit a delayed neuronal death (DND), whose mechanism is uncertain, that characterizes neurological disorders such as strokes, Alzheimer's, Huntington's and Parkinson's disease, and may mirror ischemic cell death in other tissues[1]. In survivors of cardiac arrest, transient global ischemia leads to DND of CA1 hippocampal neurons, impaired cognition and defects in memory functions within days[2,3]. These same events are recapitulated in rodents that are exposed to experimental global cerebral ischemia, which leads to DND in the hippocampus, striatum and cortex[4], and to deficits of learning and memory[5,6]. Previous research has implicated excitotoxicity as a possible mechanism of DND in the hippocampus[7], especially via activation of AMPA/kainate glutamate receptors[4].

However, there is a growing awareness that non-excitotoxic mechanisms also contribute to DND[8]. For example, in cultured neurons exposed to prolonged oxygen-glucose deprivation (OGD), treating excitotoxicity is insufficient to prevent death. This is a result, in part, of the simultaneous activation of TRPM7 channels by OGD[9]. These members of the TRP superfamily[10] comprise broadly expressed, non-selective cation channels that may affect trace ion and magnesium homeostasis[11]. When activated in hypoxic cultured neurons, TRPM7 channels elicit death independently of excitotoxicity[9]. Inhibiting these channels inhibits anoxic cell death irrespective of excitotoxicity, suggesting that TRPM7-mediated death processes may modulate or act upstream from excitotoxicity[9]. To date, the suppression of TRPM7 as

a means of studying DND mechanisms *in vivo* has not been feasible. There are currently no selective pharmacological inhibitors of this protein. Moreover, although TRPM7 inhibition by siRNA is tolerated by cultured neuronal cells[9], its deletion in DT-40B cell lines affects their survivability[12,13] and its deletion in T cells elicits dysregulated synthesis of growth factors needed for thymopoesis[14]. In addition, TRPM7 is essential for embryonic development and its global deletion in mice is lethal before day 7.5 of embryogenesis[14]. Because of this lack of viable knockout animals, concerns about adverse effects of TRPM7 deletion on cell viability and a lack of selective pharmacological blockers, the role of TRPM7 in ischemic brain damage has never been investigated.

Nonetheless, TRPM7 channels are strong candidates for mediating non-excitotoxic ischemic brain injury. Ischemia elicits large reductions in extracellular divalents, acidosis and oxidative stress[15–17], all of which are conditions that potentiate TRPM7 channels. Although they conduct only a few pA of inward current under physiological pH, extracellular calcium concentration ($[Ca^{2+}]_e$), $[Mg^{2+}]_e$ and low oxidative stress[12,18–20], TRPM7 currents increase markedly when extracellular divalents are reduced[20], as is the case in ischemia[16]. Here, we directly investigated the hypothesis that, despite the lethality of global TRPM7 deletion, these channels are important in the pathways mediating DND after ischemic injury *in vivo* and that a regional suppression of TRPM7 leads to neuronal preservation.

[1]Toronto Western Hospital Research Institute, Toronto, Ontario, Canada. [2]Department of Physiology, University of Toronto, Toronto, Ontario, Canada. [3]Robarts Research Institute, University of Western Ontario, London, Ontario, Canada. [4]Institute of Medical Science, University of Toronto, Toronto, Ontario, Canada. [5]Department of Neuroscience, Mayo Clinic, Jacksonville, Florida, USA. [6]Laboratory of Molecular Biology, Department of Synthetic Chemistry and Biological Chemistry, Graduate School of Engineering, Kyoto University, Kyoto, Japan. [7]Department of Anesthesia, Sunnybrook Health Sciences Centre, Toronto, Ontario, Canada. [8]Department of Surgery, University of Toronto, Toronto, Ontario, Canada. Correspondence should be addressed to M.T. (mike.tymianski@uhn.on.ca).
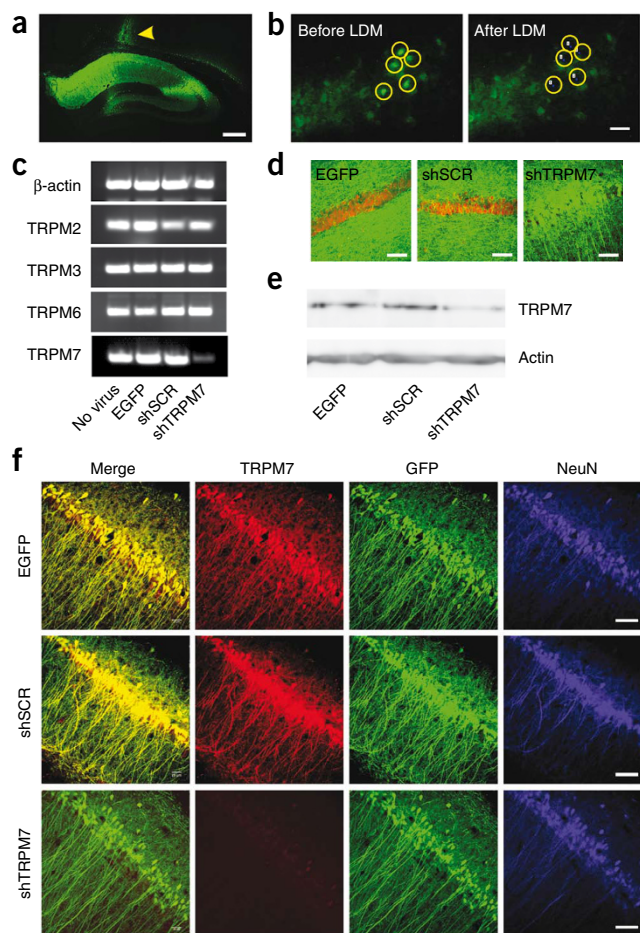
Figure 1 Suppression of TRPM7 expression in adult rat hippocampal neurons. All rats were stereotaxically injected with 7.6×10^9 genomes of rAAV vectors 10 d before analysis. (**a**) Representative EGFP fluorescence in a hippocampus injected with rAAV$_{EGFP}$. Arrowhead indicates the needle tract. Scale bar represents 500 μm. (**b**) Representative frozen section of the CA1 sector before and after laser dissection microcapture (LDM) of EGFP-positive pyramidal neurons (yellow circles) infected with rAAV$_{shTRPM7}$. Scale bar represents 25 μm. (**c**) RT-PCR of TRPM7, TRPM2, TRPM3 and TRPM6 from 60 CA1 pyramidal neurons removed by LDM as in **b** ($n = 3$ experiments). (**d**) EGFP fluorescence (green) and TRPM7 immunostaining (red) of representative frozen sections of rAAV-microinjected hippocampi used for immunoblots. Scale bar represents 75 μm. (**e**) Immunoblots of TRPM7 from hippocampal CA1 sectors infected with the indicated rAAV vectors ($n = 3$ experiments). (**f**) Immunostaining of hippocampal CA1 regions from rats infected with the indicated rAAV vectors. Scale bars represent 50 μm. Merged images show GFP and TRPM7 staining ($n = 3$ experiments).

RESULTS

TRPM7 suppression using rAAV vectors

To suppress TRPM7 in neurons, we generated a small interfering RNA (siRNA) hairpin sequence (shRNA) corresponding to coding regions 5,152–5,172 relative to the first nucleotide of the start codon of murine TRPM7 (GenBank accession number AY032951)[9] and packaged it in a recombinant serotype 1 adeno-associated virus (rAAV$_{shTRPM7}$) that included enhanced green fluorescent protein (EGFP; Online Methods, **Supplementary Notes** and **Supplementary Fig. 1**). Controls were packaged with scrambled siRNA (rAAV$_{shSCR}$) or with EGFP alone (empty vector, rAAV$_{EGFP}$). We first validated TRPM7 suppression by the rAAVs in cultured rat cortical neurons using separately validated antibodies (**Supplementary Notes** and **Supplementary Fig. 2**). Cultures were infected at 7 d *in vitro* (DIV) and studied at 14 DIV.

The vectors were highly neurotropic, infecting neurons *in vitro* with near 100% efficiency, as gauged by EGFP expression (data not shown). Infection with the rAAV$_{shTRPM7}$, but not with the control rAAVs, suppressed TRPM7 immunostaining without affecting TRPM2 expression, a related TRP channel (**Supplementary Fig. 1**). We examined TRPM2 because it and TRPM7 are unique among TRP family members in that both are stimulated by intracellular free radicals and both have been implicated in cell death[9,21]. Infecting the neurons with rAAV$_{shTRPM7}$ yielded results that were consistent with those previously obtainable by siRNA knockdown of TRPM7 (ref. 9), which rendered the cells more resistant to OGD (**Supplementary Fig. 1**, Online Methods and **Supplementary Notes**).

Suppression of TRPM7 in CA1 neurons of adult rats

We next examined whether rAAV$_{shTRPM7}$ infection *in vivo* could suppress TRPM7 in a sufficient number of cells to allow us to study cerebral ischemia. Stereotactic microinjections (7.6×10^9 genomes per injection) into the right hippocampus 10 d prior to evaluation (see Online Methods and **Supplementary Fig. 3**) produced widespread infection (**Fig. 1a** and **Supplementary Figs. 3–5**). Suppression of TRPM7 was confirmed by reverse-transcription PCR, western blots, immunostaining and electrophysiology. To avoid contamination from uninfected or non-neuronal cells, we separated neurons for RT-PCR analysis from frozen sections by laser-dissection microcapture (**Fig. 1b**). TRPM7 transcript levels were suppressed in rAAV$_{shTRPM7}$-infected cells, whereas other TRPM channel mRNA levels (TRPM2, TRPM3 and TRPM6) were unaffected (**Fig. 1c**). Next, we immunostained frozen sections from rats injected with the various rAAV vectors for TRPM7 (**Fig. 1d**). The hippocampi were dissected from sister sections in the same sample and used for immunoblots with a separately validated antibody (**Supplementary Notes** and **Supplementary Fig. 2**). We found that TRPM7 protein expression was suppressed in samples from rats treated with rAAV$_{shTRPM7}$, but not with rAAV$_{shSCR}$ or rAAV$_{EGFP}$ (**Fig. 1e**). These samples contained proteins pooled from both neuronal (rAAV infected) and non-neuronal (uninfected) hippocampal cells, and may overestimate the relative amounts of TRPM7 protein remaining in the neurons. Consistent with our *in vitro* results (**Supplementary Fig. 1**), the rAAV vectors had no apparent effect on neuronal morphology. However, treatment with rAAV$_{shTRPM7}$ attenuated TRPM7 immunostaining in hippocampal CA1 neurons (**Fig. 1f**).

Induction of RNAi in mammalian cells by expression of double-stranded RNA can activate innate antiviral (interferon) response pathways that may elicit off-target gene expression[22,23]. Therefore, we confirmed that the rAAV vectors did not activate interferon target genes (**Supplementary Notes** and **Supplementary Fig. 2**). We then addressed the concern that TRPM7 may be needed for the survival of certain mammalian cells[12,13,24] and that its suppression *in vivo* could reduce neuronal viability and complicate the interpretation of functional and stroke experiments involving DND. We counted the EGFP-positive CA1 pyramidal neurons in six coronal planes at 7, 10 and 14 d after rAAV infection (**Supplementary Figs. 3–5**). Rats infected with rAAV$_{shTRPM7}$ had similar numbers of EGFP-positive CA1 pyramidal neurons as those infected with control vectors, suggesting that suppressing TRPM7 *in vivo* does not affect basal neuronal viability (**Fig. 2a** and **Supplementary Figs. 3–5**).
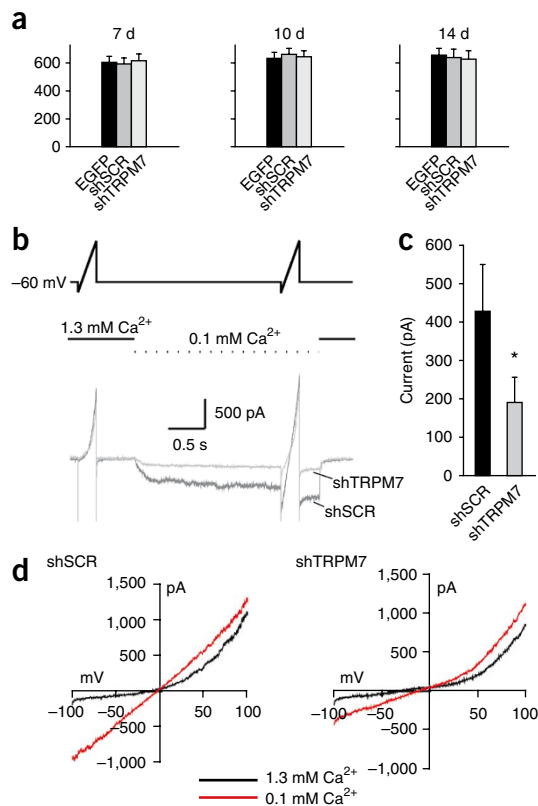
To evaluate the downregulation of TRPM7 function by the rAAVs, we carried out whole-cell patch-clamp recordings from acutely

Figure 2 Suppression of TRPM7 is well tolerated *in vivo*. (**a**) Counts of EGFP-positive CA1 neurons in hippocampi infected with the indicated rAAV vectors at the indicated days post-microinjection (*n* = 6 rats per group, mean ± s.e.m.). (**b**) Representative traces of the response of acutely isolated CA1 neurons (dark gray, rAAV$_{shSCR}$-infected neuron; light gray, rAAV$_{shTRPM7}$-infected neuron) to a 5-s application of ECS containing 0.1 mM Ca^{2+}. The top and middle traces show the timing of the applied voltage ramps (±100 mV, 500 ms) and of solution exchange, respectively. (**c**) Summary of peak currents from each of the treatment groups (shSCR, *n* = 10; shTRPM7, *n* = 7). Currents evoked by 0.1 mM Ca^{2+} were smaller in shTRPM7-infected than in shSCR-infected neurons (* indicates *P* < 0.05, two-tailed Student's *t* test for unpaired samples, mean ± s.e.m.). (**d**) Current-voltage relations derived from the voltage ramps in **b** applied to neurons from rats infected with shSCR (left) or shTRPM7 (right) rAAVs in ECS containing 1.3 mM (black) or 0.1 mM (red) Ca^{2+}. Consistent with the suppression of TRPM7 expression, current rectification was almost entirely abolished in neurons expressing shSCR, but not in those expressing shTRPM7, when the extracellular Ca^{2+} concentration was reduced to 0.1 mM.

extracellular Ca^{2+} and/or Mg^{2+} transiently evokes an inward cation current[25,26]. This current is at least partly mediated by TRPM7, as determined previously using the shRNA/siRNA sequence to TRPM7 that we used here. When delivered into cultured hippocampal neurons using adenoviral vectors, this shRNA reduces both TRPM7 mRNA levels and low $[Ca^{2+}]_e$-evoked currents[20]. The siRNA sequence, when transfected into cultured cortical neurons by conventional means, inhibits anoxia-evoked TRPM7-dependent currents[9].

In the acutely dissociated neurons taken from rAAV$_{SCR}$-infected rats, we evoked a current using a 5-s application of extracellular solution (ECS) containing 0.1 mM Ca^{2+} (**Fig. 2b**). The amplitude of the low $[Ca^{2+}]_e$-evoked current was attenuated in neurons infected with rAAV$_{shTRPM7}$ (**Fig. 2b,c**), which is consistent with TRPM7 inhibition. Furthermore, TRPM7-mediated currents have an outwardly rectifying *I-V* curve that is lost when extracellular divalent

isolated hippocampal neurons from 4–5-week-old rats that were given intrahippocampal injections of rAAV$_{shTRPM7}$ or rAAV$_{shSCR}$ at 3 weeks of age. In acutely isolated hippocampal neurons and in neurons grown in dissociated cell cultures, lowering the concentration of

Figure 3 TRPM7 suppression *in vivo* imparts resilience to DND. (**a**) Representative coronal images of neurons and dendrites derived from hippocampi of rats infected with the indicated rAAV vector 7 d before a 15-min 4VO. Brains were cryostat sectioned (25 μm) and imaged 72 h after the ischemic insult. Images are representative of 6 rats per group. (**b**) Representative images taken from rats infected with the indicated rAAV vectors and undergoing sham surgery under otherwise identical conditions to those described in **a**. Scale bars in **a** and **b** represent 200, 50, 20 and 10 μm for images taken with ×3.5, ×25, ×63 and ×126 power objectives, respectively (×126 power was obtained with a ×63 objective and a ×2 digital gain). (**c**) Representative coronal sections of TUNEL-staining in the CA1 sectors of hippocampi of a rat injected with rAAV$_{shTRPM7}$ 7 d before 4VO. The hippocampus ipsilateral (right) and contralateral (left) to the injection is shown, stained 3 d after 4VO (representative of 6 rats). (**d**) Counts (see Online Methods) of TUNEL-stained CA1 neurons as in **c** from the ipsilateral (rAAV-microinjected) and contralateral (uninjected) hippocampus (*n* = 6 rats per group). * indicates difference from all other groups (ANOVA, *P* < 0.002; Fisher LSD test, shTRPM7 injected versus contralateral, *P* < 0.001). (**e**) Counts (mean ± s.e.m.) of EGFP-expressing CA1 neurons from the 4VO experiment represented in **a** (4VO, *n* = 6 rats per group; sham, 3 rats per group). ** indicates difference from shTRPM7 and sham groups (ANOVA, *P* < 0.01; Fisher LSD test, EGFP versus shTRPM7, *P* < 0.001; shSCR versus shTRPM7, *P* < 0.001; EGFP versus shSCR, *P* = 0.378).
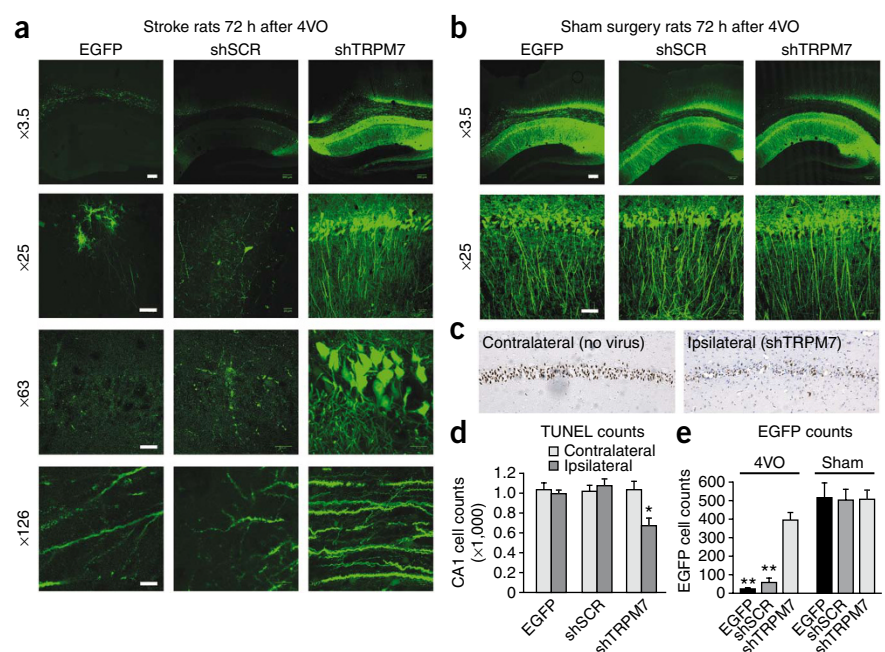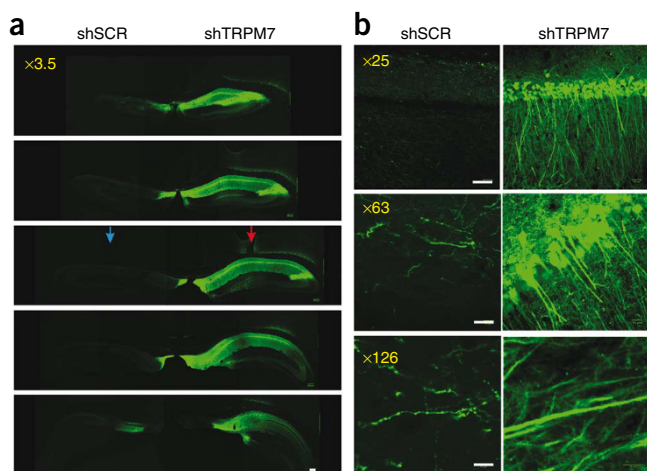
Figure 4 Persistent resilience of TRPM7-deficient hippocampi to ischemia 7 d post 4VO. Rats were microinjected with the rAAV$_{shSCR}$ and rAAV$_{shTRPM7}$ in the left and right hippocampus, respectively, 7 d before 4VO. (**a**) Five coronal hippocampal sections taken from a representative rat 7 d after 4VO. Arrows indicate injection sites of rAAV$_{shSCR}$ (blue) and rAAV$_{shTRPM7}$ (red). (**b**) Representative higher-magnification images of neurons and dendrites from the same rat. Scale bars in **a** and **b** represent 200, 50, 20 and 10 µm for images taken with ×3.5, ×25, ×63 and ×126 power objectives, respectively.

are reduced[20]. Consistent with this, application of ECS containing 0.1 mM Ca^{2+} almost entirely abolished rectification in neurons infected with rAAV$_{shSCR}$, but not with the rAAV$_{shTRPM7}$, providing further evidence that TRPM7 function was downregulated (**Fig. 2d**).

To further evaluate neuronal viability and function after rAAV infection, we carried out electrophysiological recordings from brain slices derived from adult rats infected 10 d previously with the vectors. After the recordings, we immunostained slices to confirm TRPM7 suppression (**Supplementary Fig. 6**). The loss of TRPM7 had no effect on short-term plasticity that was elicited immediately after high-frequency stimulation (HFS, data not shown), LTP in the CA1 region (**Supplementary Fig. 6**), input/output relationships (**Supplementary Fig. 7**) or short-term plasticity of glutamatergic transmission, as tested using field recordings
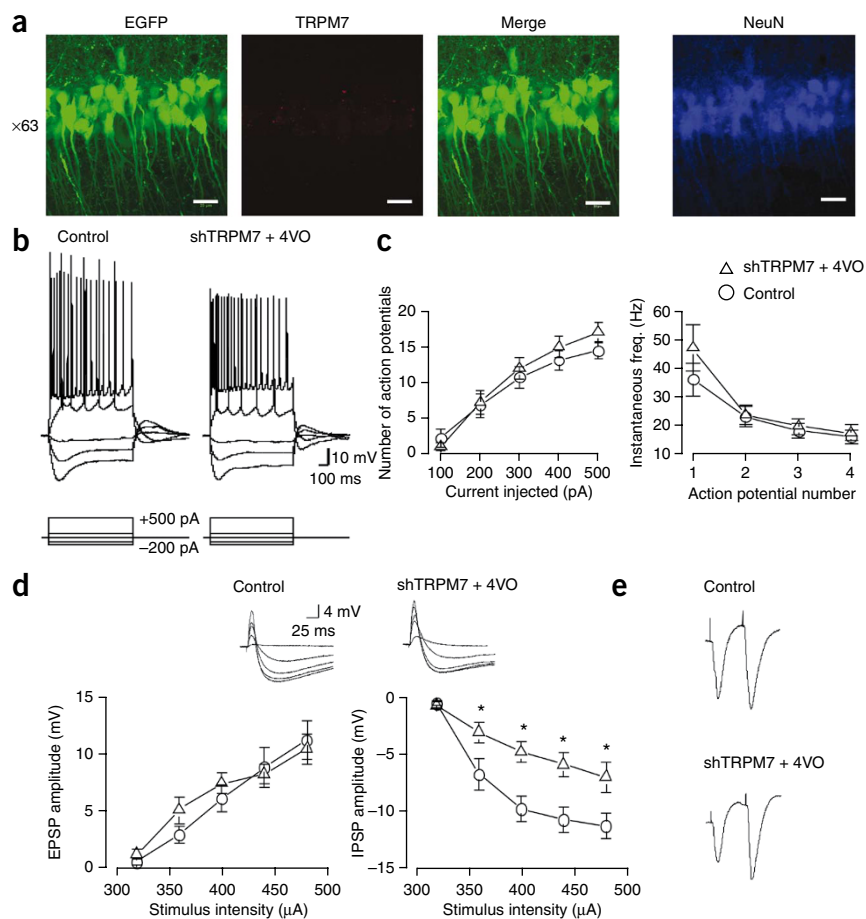
and a paired-pulse procedure (**Supplementary Fig. 8**). Thus, TRPM7 suppression in the CA1 *in vivo* is compatible with the continued survival and functionality of the affected neurons.

## TRPM7 suppression inhibits ischemic DND in CA1 neurons

We next examined the role of TRPM7 in DND in the hippocampus following transient global cerebral ischemia. Global cerebral ischemia produces CA1 neuronal death within 24–72 h[27,28] and causes longstanding memory deficits in rats[5,6] and humans[2,3]. DND after global cerebral ischemia is partially responsive to treatment using several strategies, including anti-excitotoxic or antioxidant agents[7,29]. However, studies of cultured neurons that undergo hypoxia have suggested that TRPM7 activity potentiates oxidative pathways and promotes cell death even when excitotoxicity is blocked[9]. To test whether TRPM7 participates in DND, we stereotaxically microinjected the rAAV$_{EGFP}$, rAAV$_{shSCR}$ or rAAV$_{shTRPM7}$ vectors into the right hippocampus as described above ($n = 6$ rats per group). After 7 d, the rats were subjected to a transient (15 min) episode of forebrain ischemia

Figure 5 Persistence of function in surviving TRPM7-deficient CA1 neurons 30 d after ischemia. Recordings were made from brain slices obtained 30 d after 4VO from rats previously microinjected with rAAV$_{shTRPM7}$ and from age-matched (nonischemic) controls. (**a**) Direct EGFP, TRPM7 and NeuN immunofluorescence from the CA1 sector of a hippocampal slice taken from a representative rAAV$_{shTRPM7}$-infected rat and stained post recording, confirming neuronal preservation and lack of TRPM7 staining at 30 d. Scale bar represents 20 µm. (**b**) Superimposed representative traces illustrating the responsiveness of neurons to the indicated series of current steps. (**c**) Similar response of the two neuronal populations ($n = 8$ per group) to increasing depolarizing current intensity (+100 to +500 pA) with respect to the number of action potentials fired (left) and spike-frequency accommodation (right). (**d**) Excitatory postsynaptic potential (EPSP, left) and IPSP (right) amplitude response of the two neuronal populations ($n = 8$ per group) to the indicated stimulus intensity. * indicates difference from controls ($P < 0.05$, two-way ANOVA with Bonferroni post-test). Inset: representative EPSP-IPSP traces. Error bars are s.e.m. (**e**) Representative traces illustrating unaltered paired-pulse facilitation of EPSCs.
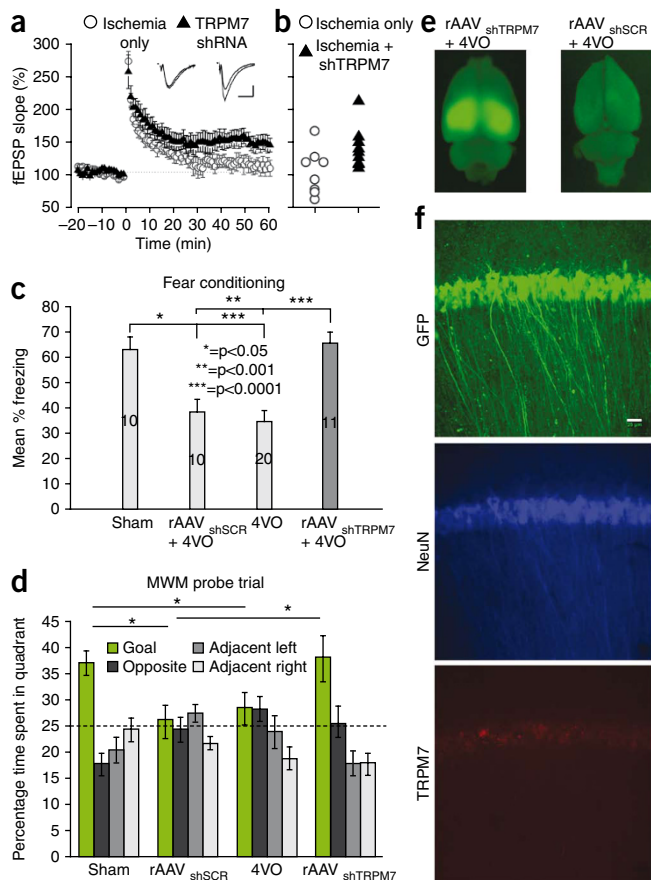
Figure 6 TRPM7 deficiency prevents loss of memory functions in rats subjected to global ischemia. (**a**,**b**) LTP was preserved in TRPM7-deficient hippocampi derived from rats subjected to ischemia. A summary of the LTP experiments in slices obtained ~30 d after 4VO in rats previously microinjected with rAAV$_{shTRPM7}$ (filled triangles, $n = 9$) or in post-ischemic, uninjected age-matched controls (open circles, $n = 8$) is shown in **a**. Synaptic responses recorded during the last 5 min after LTP induction were averaged and compared using Student's t test (unpaired, two-tailed). The differences between the two groups were significant ($P < 0.05$). Within each treatment group, the distribution of normalized fEPSP slope values, recorded 60 min after HFS, was plotted for each slice (**b**). LTP at $t = 60$ min, defined as an increase in normalized fEPSP of greater than two s.e.m. above baseline, was induced in 9 out of 9 slices from rAAV$_{shTRPM7}$-treated rats, but in only 4 out of 8 slices in ischemia-only rats. (**c**,**d**) Rats that underwent bilateral hippocampal injections of rAAVs and control rats were subjected to behavioral assays designed to test hippocampal-dependent memory. The results of constitutional fear conditioning 14 d after 4VO are shown in **c**. The numbers of rats per group are indicated in the bars. Probe trial performance in the MWM 11 d post-ischemia is shown in **d**. Rats underwent sham surgery, 4VO or 4VO 7d after microinjection of the indicated vector ($n = 20$ rats per group). * indicates $P < 0.05$. (**e**) Whole-brain EGFP fluorescence of representative rats that were tested in the MWM in **d**, at 30 d post 4VO. (**f**) Representative immunofluorescence sections of the CA1 sector of the shTRPM7-treated rat in **e**. Scale bar represents 25 μm. Error bars in **a**, **c** and **d** represent s.e.m.

($n = 6$ ischemia rats per rAAV vector group) and processed the rat brains for terminal deoxynucleotidyl transferase dUTP nick-end labeling (TUNEL)[33]. TUNEL stains cells with DNA fragmentation, irrespective of cell type or whether they were infected by the vectors. Blinded cell counts revealed that hippocampi treated with the rAAV$_{shTRPM7}$ vector had about 30% fewer TUNEL-positive cells as compared with the contralateral side or with rAAV$_{EGFP}$- and rAAV$_{shSCR}$-treated rats (**Fig. 3c,d**). Unlike our counts of EGFP-stained neurons, these TUNEL counts reflect the staining of fragmented DNA in uninfected neurons, activated astrocytes and microglia/macrophages, which accounted for up to 40% of TUNEL-stained cells 72 h after 4VO (**Supplementary Fig. 10**). These results indicate that global ischemia also affected cells that were not infected by the vectors and illustrate that selectively protecting hippocampal CA1 cells using a neurotropic vector–based approach does not prevent all TUNEL-detectable DNA fragmentation in the post-ischemic hippocampus.

Because both hippocampi are rendered equally ischemic in the 4VO model, we next compared ischemic neuronal survival after microinjection of rAAV$_{shTRPM7}$ and rAAV$_{shSCR}$ into the right and left hippocampus, respectively (**Fig. 4a**). We microinjected rats with the vectors 7 d before administering a 15-min 4VO ischemic insult ($n = 6$). Brain slices derived from the rats were examined 7 d later and we found that neuronal and dendritic morphology were preserved in the hippocampi injected with rAAV$_{shTRPM7}$, but not in the rAAV$_{shSCR}$-treated hippocampi (**Fig. 4a,b**). We counted the surviving (EGFP expressing) CA1 neurons and found that the rAAV$_{shTRPM7}$-treated ischemic hippocampi retained neurons in numbers that were comparable (allowing for variability in counts between non-concurrent experiments) to those present in nonischemic infected brains (586.5 ± 134.84 and 14.67 ± 7.98 for rAAV$_{shTRPM7}$ and rAAV$_{shSCR}$ rats, respectively; Student's t test, $P < 0.002$).

TRPM7 suppression enhances recovery post ischemia

To examine the effect of TRPM7 suppression on the functionality of surviving cells, we examined the electrophysiological properties of CA1 neurons in brain slices taken from post-ischemic rats infected with rAAV$_{shTRPM7}$ 7 d before 4VO. The extensive hippocampal

using the 4-vessel occlusion technique (4VO; see Online Methods)[27] and then allowed to recover for 72 h. We subjected sham controls (3 rats per group) to the same protocol, but without ischemia. Brain sections derived from the rats were examined to assess the survival and morphology of hippocampal neurons (**Fig. 3**). Ischemic rats treated with the rAAV$_{EGFP}$ or rAAV$_{shSCR}$ vectors showed an extensive, progressive loss of EGFP expression in the hippocampus (**Fig. 3a** and **Supplementary Fig. 9**). The EGFP loss is consistent with a turnover of existing EGFP ($t_{1/2}$ of ~24 h)[30] and inhibition of protein synthesis in global ischemia[7]. The latter is attributable to phosphorylation of the alpha subunit of eukaryotic initiation factor 2, as demonstrated in our rats (**Supplementary Fig. 9**), and leads to failure of translation initiation[31]. The remaining EGFP-labeled neurons showed dendritic beading, compaction and reduced dendrite density in all of the CA1 areas that we examined (**Fig. 3a**). In contrast, the hippocampi of ischemic rats infected with rAAV$_{shTRPM7}$ robustly expressed EGFP, indicating that the neurons were viable and that the dendritic structures were preserved (**Fig. 3a**). We used a blinded observer to count the number of CA1 cells expressing EGFP, which reflect living infected neurons, and found significant preservation of EGFP-expressing CA1 neurons in the rAAV$_{shTRPM7}$-treated rats, but not in those treated with control rAAVs ($P < 0.01$; **Fig. 3e**). CA1 neuronal numbers and dendritic structures were preserved in sham controls (no ischemia) throughout the observation period (**Fig. 3b,e**).

EGFP expression is only a marker for neurons infected by the neurotropic rAAVs. However, ischemia causes astrocyte and microglial activation and inflammatory cell migration, which peak in the affected area around 3–4 d post-ischemia[32]. To determine whether uninfected cells were also protected, we repeated these experiments

damage sustained by post-ischemic rats treated with rAAV$_{shSCR}$ or rAAV$_{EGFP}$ prevented us from obtaining stable recordings. Therefore, the data from rAAV$_{shTRPM7}$-treated rats were compared to those from uninfected nonischemic controls. Whole-cell currents and field recordings were difficult to obtain in rAAV$_{shTRPM7}$-treated slices taken 7–14 d post ischemia, suggesting that the surviving cells were still fragile or metabolically compromised. At 30 d post-ischemia, however, we easily obtained whole-cell current- and voltage-clamp recordings (**Supplementary Notes**) and a robust EGFP fluorescence in the rAAV$_{shTRPM7}$-treated CA1 neurons indicated that shRNA construct expression persisted and demonstrated the long-term survivability of the neurons (**Fig. 5a**). TRPM7-deficient neurons surviving the ischemic insult had a normal capacity to fire action potentials and had normal spike-frequency adaptation (**Fig. 5b,c**). Surviving TRPM7-deficient neurons also maintained dendritic function, as suggested by the preservation of excitatory and inhibitory synaptic current and our observation of spontaneous excitatory and inhibitory postsynaptic currents (**Fig. 5d** and **Supplementary Notes**). We observed a depression of inhibitory postsynaptic potential (IPSP) amplitudes in surviving TRPM7-deficient neurons (**Fig. 5d**). The mechanism underlying such depression remains unclear and could reflect potential modification of GABA$_A$ receptor expression or function, reduced excitatory drive onto interneurons, or, alternatively, an injury to interneurons. The neurons showed unaltered paired-pulse facilitation of excitatory postsynaptic currents (EPSCs; pulse 2/pulse 1 ratios were 1.41 ± 0.08 and 1.51 ± 0.10 in neurons of control and rAAV$_{shTRPM7}$ + 4VO rats, respectively; $n = 8$ per group), suggesting that presynaptic function is normal (**Fig. 5e**). Thus, with the exception of evoked IPSPs, intrinsic membrane properties and synaptic responses in post-ischemic TRPM7-deficient neurons were largely indistinguishable from those of nonischemic controls, suggesting that these cells were functionally preserved (see **Supplementary Table 1** and **Supplementary Notes**).

Certain forms of memory require intact hippocampal neuronal networks[34,35]. We next determined whether the functional neuronal preservation that we observed during TRPM7 suppression (**Fig. 5**) would translate into a capacity to induce LTP in the hippocampal CA1 area by HFS. LTP induction by HFS has been the primary model used to study the cellular and molecular basis of memory[35,36]. For these experiments, we bilaterally injected rAAV$_{shTRPM7}$ into the rats' hippocampus. Controls underwent sham injection (no rAAV infection) and all of the rats were subjected to ischemia by 4VO 7 d later. We measured LTP, paired-pulse responses and input-output functions in brain slices taken from rats in each group 30 d after the 4VO procedure. We found no changes in paired-pulse responses or input-output functions in these recordings (data not shown). However, rats that had undergone TRPM7 suppression in the hippocampus before ischemia had a greater capacity for LTP as compared with rats that experienced ischemia alone (**Fig. 6a,b**). Synaptic response recording during the last 5 min after LTP induction confirmed a significant difference between the TRPM7-deficient and the ischemia-only groups ($P < 0.05$).

Consistent with the human situation[2,3], 4VO in rats leads to behavioral consequences, mainly in the performance of learning and memory tasks[5,6]. To determine whether these were preserved post-ischemia by TRPM7 suppression, we subjected the rats to two behavioral assays that test hippocampal-dependent memory: a contextual fear conditioning procedure[37] and the fixed platform version of the Morris water maze (MWM)[38]. We carried out bilateral hippocampal injections of rAAV$_{shTRPM7}$ or rAAV$_{shSCR}$, followed 7 d later by 4VO. Additional controls underwent 4VO without rAAV infection or sham surgery (no ischemia or rAAV infection). To study the rats' ability to

learn and remember an association between an adverse experience and environmental cues, we evaluated contextual fear conditioning at 14 d post-ischemia (Online Methods). All of the groups had similar freezing scores before conditioning (data not shown). The freezing scores of the rAAV$_{shTRPM7}$ + 4VO group were similar to those of sham-operated (non-ischemic) rats 24 h after conditioning ($P > 0.05$; **Fig. 6c**), and those scores were higher than those of the rAAV$_{shSCR}$ + 4VO rats ($P < 0.05$) and 4VO only controls ($P < 0.001$; **Fig. 6c**). Thus, 4VO impaired the acquisition of contextual fear memory, whereas TRPM7 suppression preserved fear memory performance post-ischemia.

The MWM test of spatial navigation measures the ability of the rat to learn and remember a location defined by its position relative to distal extramaze cues. We subjected the rats to MWM learning acquisition trials for 5 consecutive days (7–11 d post-ischemia; Online Methods) 7 d after 4VO. A probe trial that measured the ability to locate the quadrant that previously contained the hidden platform was carried out 4 h after the final acquisition trial on day 5. The rate of task acquisition was initially slowed in all of the groups subjected to ischemia, as evidenced by the increased time to find the hidden platform (**Supplementary Fig. 11**). There was no evidence of impaired motor performance, as indicated by unaffected swim speeds on any of the days of testing or the probe trial (**Supplementary Fig. 11**). However, the impairment in spatial memory demonstrated during the probe trial was only observed in uninfected post-ischemic rats and in post-ischemic rats infected with rAAV$_{shSCR}$. Post-ischemic rats deficient in TRPM7 performed similarly to sham surgery rats in remembering the quadrant that previously contained the hidden platform (**Fig. 6d**), indicating that their capacity to learn the task was preserved, as was their memory performance. Examination of the brains revealed that GFP fluorescence persisted (**Fig. 6e,f**) and that TRMP7 was suppressed (as shown by immunoreactivity), indicating continued construct expression in the tested rats (**Fig. 6f**, compare with **Fig. 1f**).

DISCUSSION

Collectively, our data show that TRPM7 suppression in hippocampal CA1 neurons *in vivo* is well tolerated, imparts resilience to ischemic damage, and preserves neuronal function and performance for hippocampus-dependent learning tasks after ischemic brain injury. Although our prior work has implicated TRPM7 in the anoxic death of cultured neurons[9], other studies have suggested that over- or under-expressing TRPM7 may have adverse consequences. For example, its overexpression leads to the death of HEK-293 cells[12], its disruption affects the survival of cultured DT-40B cells[12,13] and its deletion in T cells elicits dysregulated synthesis of growth factors that are necessary for thymopoesis[14]. TRPM7 is also essential for embryonic development and its global deletion in mice is lethal[14]. To the best of our knowledge, our results are the first demonstration that suppressing TRPM7 in adult mammals is feasible and that this markedly reduces delayed neuronal death after ischemia. Thus, there is a possibility that TRPM7 can be selectively targeted to prevent ischemic brain damage.

Recently, we demonstrated that TRPM7 channels in cultured CA1 neurons may act as extracellular detectors of divalent cation levels[20]. Tissue ischemia *in vivo* causes a reduction in extracellular Ca^{2+} and Mg^{2+} concentrations[16,17] and such conditions enhance TRPM7 currents[20]. Thus, ischemia may promote ionic circumstances that are compatible with TRPM7 overactivity. In cultures, such overactivity leads to free and total intracellular calcium overload, which results in nitric oxide production, oxidative stress and cell death. These

ARTICLES

mechanisms are similar to those previously attributed to excitotoxicity, but are now known to occur even if excitotoxicity and other known Ca^{2+} influx pathways are pharmacologically blocked[9]. Moreover, excitotoxicity may be self-limiting, as glutamate receptors desensitize and anoxic cell membranes depolarize, and this leads to reductions in spontaneous activity and neurotransmitter release[9]. Consequently, TRPM7 proteins may govern cell death pathways that can be triggered independently of excitotoxicity, but converge on similar downstream injurious pathways. If so, then anti-excitotoxic therapy may be insufficient for treating ischemic brain damage in stroke or other conditions involving DND[39,40].

Our report supports an increasing body of literature that describes non-excitotoxic mechanisms of neuronal death, including those involving TRP channels[9,21], acid-sensing channels[41] and hemichannels[42]. Our finding that TRPM7 channels mediate DND in brain ischemia identifies these proteins and their downstream signaling pathways as targets for future research. However, our use of siRNA to regionally inhibit TRPM7 is limited by several uncertainties. First, the functional role of TRPM7 channels in CA1 neurons is still poorly understood. Although we have demonstrated that they may act as divalent cation sensors in cultured hippocampal neurons[20], the physiological purpose of this is incompletely understood, as is the effect of these observations on neuronal function. The rAAV approach only enhanced the resilience of a subset of cells (infected neurons) and this may need to be improved to treat other cell types affected by brain ischemia. The siRNA approach was insufficient to fully elucidate the functional role of TRPM7 channels in neurons, and such future research will require, among others, the development of specific pharmacological inhibitors for ion channel studies. A further uncertainty of the use of siRNA is the inability of this approach to completely block a protein's expression or function. This raises the possibility that, although complete global deletion of TRPM7 is lethal[14], a partial suppression may be well tolerated and would not require a regional strategy. However, in the absence of specific pharmacological inhibitors of TRPM7, this possibility remains to be tested. Further experiments are warranted to determine whether the effect of TRPM7 suppression lasts beyond the times that we examined and whether the effects that we observed involve the preservation of original cells, enhanced neurogenesis, plasticity or other means by which TRPM7 suppression might improve outcome. Lastly, the chronic nature of TRPM7 suppression by RNAi raises the possibility that its partial deletion causes sublethal stress that induces unknown signals that induce an ischemia-resistant state.

Although TRPM7 is thought to be important for cellular trace ion and Mg^{2+} homeostasis under certain circumstances[11,13], its deletion in thymocytes disrupts thymopoiesis, but does not affect acute uptake of Mg^{2+} or the maintenance of total cellular Mg^{2+} (ref. 14). It is possible that diverse cell types have different dependencies on TRPM7 or different redundant mechanisms that compensate for this protein's functions. Nevertheless, our results provide a rationale for developing pharmacologic means of targeting TRPM7 channels to further study their physiological and pathological roles *in vitro* and *in vivo* and to inhibit ischemic damage. The knowledge that these channels are broadly expressed in vertebrate tissues should not dissuade such research. Many commonly used drugs, such as calcium channel blockers for the treatment of hypertension, also target widely expressed proteins, but are now in commonly used in humans. Instead, the awareness of the broad expression of TRPM7 channels in and outside the CNS raises the possibility that they might also participate in other neurodegenerative disorders, as well as in ischemic mechanisms of other tissues in which they are found.

METHODS

Methods and any associated references are available in the online version of the paper at http://www.nature.com/natureneuroscience/.

Note: Supplementary information is available on the Nature Neuroscience website.

AUTHOR CONTRIBUTIONS
H.-S.S. carried out the stereotactic rAAV infections, sectioning, immunochemistry, imaging, cell counts, laser dissection microcapture and PCR. K.J. and T.E.G. designed and manufactured the rAAV vectors, M.F.J. and J.F.M. performed the electrophysiology experiments, L.T. carried out the 4VO and histology procedures, Y.M. generated the antibodies to TRPM7, S.K. and H.C. performed the immunoblots, M.J. carried out the TUNEL cell counts, and J.P.F., M.J., H.C. and H.-S.S. performed the OGD experiments. L.J.M. and B.A.O. carried out the neurobehavioral evaluations. M.T. and H.-S.S. wrote the paper. All authors discussed the results and commented on the manuscript.

Published online at http://www.nature.com/natureneuroscience/.
Reprints and permissions information is available online at http://www.nature.com/reprintsandpermissions/.

1. Hausenloy, D.J. & Scorrano, L. Targeting cell death. *Clin. Pharmacol. Ther.* **82**, 370–373 (2007).
2. Volpe, B.T. & Petito, C.K. Dementia with bilateral medial temporal lobe ischemia. *Neurology* **35**, 1793–1797 (1985).
3. Petito, C.K., Feldmann, E., Pulsinelli, W.A. & Plum, F. Delayed hippocampal damage in humans following cardiorespiratory arrest. *Neurology* **37**, 1281–1286 (1987).
4. Bennett, M.V. *et al.* The GluR2 hypothesis: Ca^{2+}-permeable AMPA receptors in delayed neurodegeneration. *Cold Spring Harb. Symp. Quant. Biol.* **61**, 373–384 (1996).
5. Volpe, B.T., Pulsinelli, W.A., Tribuna, J. & Davis, H.P. Behavioral performance of rats following transient forebrain ischemia. *Stroke* **15**, 558–562 (1984).
6. Block, F. Global ischemia and behavioral deficits. *Prog. Neurobiol.* **58**, 279–295 (1999).
7. Lipton, P. Ischemic cell death in brain neurons. *Physiol. Rev.* **79**, 1431–1568 (1999).
8. Besancon, E., Guo, S., Lok, J., Tymianski, M. & Lo, E.H. Beyond NMDA and AMPA glutamate receptors: emerging mechanisms for ionic imbalance and cell death in stroke. *Trends Pharmacol. Sci.* **29**, 268–275 (2008).
9. Aarts, M. *et al.* A key role for TRPM7 channels in anoxic neuronal death. *Cell* **115**, 863–877 (2003).
10. Montell, C., Birnbaumer, L. & Flockerzi, V. The TRP channels, a remarkably functional family. *Cell* **108**, 595–598 (2002).
11. Monteilh-Zoller, M.K. *et al.* TRPM7 provides an ion channel mechanism for cellular entry of trace metal ions. *J. Gen. Physiol.* **121**, 49–60 (2003).
12. Nadler, M.J. *et al.* LTRPC7 is a Mg.ATP-regulated divalent cation channel required for cell viability. *Nature* **411**, 590–595 (2001).
13. Schmitz, C. *et al.* Regulation of vertebrate cellular Mg^{2+} homeostasis by TRPM7. *Cell* **114**, 191–200 (2003).
14. Jin, J. *et al.* Deletion of Trpm7 disrupts embryonic development and thymopoiesis without altering Mg^{2+} homeostasis. *Science* **322**, 756–760 (2008).
15. Siesjo, B.K., Katsura, K. & Tibor, K. Acidosis related brain damage. in *Advances in Neurology: Cellular and Molecular Mechanisms of Ischemic Brain Damage* (eds. Siesjo, B.K. & Wieloch, T.) (Raven Press, New York, 1994).
16. Silver, I.A. & Erecinska, M. Intracellular and extracellular changes of $[Ca^{2+}]$ in hypoxia and ischemia in rat brain *in vivo*. *J. Gen. Physiol.* **95**, 837–866 (1990).
17. Lin, M.C. *et al.* Microdialysis analyzer and flame atomic absorption spectrometry in the determination of blood glucose, lactate and magnesium in gerbils subjected to cerebral ischemia/reperfusion. *J. Am. Coll. Nutr.* **23**, 556S–560S (2004).
18. Runnels, L.W., Yue, L. & Clapham, D.E. TRP-PLIK, a bifunctional protein with kinase and ion channel activities. *Science* **291**, 1043–1047 (2001).
19. Kozak, J.A., Kerschbaum, H.H. & Cahalan, M.D. Distinct properties of CRAC and MIC channels in RBL cells. *J. Gen. Physiol.* **120**, 221–235 (2002).
20. Wei, W.L. *et al.* TRPM7 channels in hippocampal neurons detect levels of extracellular divalent cations. *Proc. Natl. Acad. Sci. USA* **104**, 16323–16328 (2007).
21. Kaneko, S. *et al.* A critical role of TRPM2 in neuronal cell death by hydrogen peroxide. *J. Pharmacol. Sci.* **101**, 66–76 (2006).
22. Bridge, A.J., Pebernard, S., Ducraux, A., Nicoulaz, A.L. & Iggo, R. Induction of an interferon response by RNAi vectors in mammalian cells. *Nat. Genet.* **34**, 263–264 (2003).

23. Sledz, C.A., Holko, M., de Veer, M.J., Silverman, R.H. & Williams, B.R. Activation of the interferon system by short-interfering RNAs. *Nat. Cell Biol.* **5**, 834–839 (2003).
24. Schmitz, C. *et al.* The channel kinases TRPM6 and TRPM7 are functionally nonredundant. *J. Biol. Chem.* **280**, 37763–37771 (2005).
25. Xiong, Z.G., Chu, X.P. & MacDonald, J.F. Effect of lamotrigine on the Ca^{2+}-sensing cation current in cultured hippocampal neurons. *J. Neurophysiol.* **86**, 2520–2526 (2001).
26. Xiong, Z., Lu, W. & MacDonald, J.F. Extracellular calcium sensed by a novel cation channel in hippocampal neurons. *Proc. Natl. Acad. Sci. USA* **94**, 7012–7017 (1997).
27. Pulsinelli, W.A. & Brierly, J.B. A new model of bilateral hemispheric ischemia in the unanesthetized rat. *Stroke* **10**, 267–272 (1979).
28. Pulsinelli, W.A., Brierly, J.B. & Plum, F. Temporal profile of neuronal damage in a model of transient forebrain ischemia. *Ann. Neurol.* **11**, 491–498 (1982).
29. Saito, A. *et al.* Oxidative stress and neuronal death/survival signaling in cerebral ischemia. *Mol. Neurobiol.* **31**, 105–116 (2005).
30. Corish, P. & Tyler-Smith, C. Attenuation of green fluorescent protein half-life in mammalian cells. *Protein Eng.* **12**, 1035–1040 (1999).
31. Kumar, R. *et al.* Brain ischemia and reperfusion activates the eukaryotic initiation factor 2α kinase, PERK. *J. Neurochem.* **77**, 1418–1421 (2001).
32. Stoll, G., Jander, S. & Schroeter, M. Inflammation and glial responses in ischemic brain lesions. *Prog. Neurobiol.* **56**, 149–171 (1998).
33. Gavrieli, Y., Sherman, Y. & Ben-Sasson, S.A. Indentification of programmed cell death in situ via specific labeling of nuclear DNA fragmentation. *J. Cell Biol.* **119**, 493–501 (1992).
34. Ji, J. & Maren, S. Hippocampal involvement in contextual modulation of fear extinction. *Hippocampus* **17**, 749–758 (2007).
35. Whitlock, J.R., Heynen, A.J., Shuler, M.G. & Bear, M.F. Learning induces long-term potentiation in the hippocampus. *Science* **313**, 1093–1097 (2006).
36. Lisman, J., Schulman, H. & Cline, H. The molecular basis of CaMKII function in synaptic and behavioral memory. *Nat. Rev. Neurosci.* **3**, 175–190 (2002).
37. Fanselow, M.S. Conditioned and unconditional components of post-shock freezing. *Pavlov. J. Biol. Sci.* **15**, 177–182 (1980).
38. Morris, R. Developments of a water-maze procedure for studying spatial learning in the rat. *J. Neurosci. Methods* **11**, 47–60 (1984).
39. Morris, G.F. *et al.* Failure of the competitive N-methyl-D-aspartate antagonist Selfotel (CGS 19755) in the treatment of severe head injury: results of two phase III clinical trials. The selfotel investigators. *J. Neurosurg.* **91**, 737–743 (1999).
40. Davis, S.M., Albers, G.W., Diener, H.C., Lees, K.R. & Norris, J. Termination of acute stroke studies involving selfotel treatment. ASSIST steering committed. *Lancet* **349**, 32 (1997).
41. Xiong, Z.G. *et al.* Neuroprotection in ischemia: blocking calcium-permeable acid-sensing ion channels. *Cell* **118**, 687–698 (2004).
42. Thompson, R.J., Zhou, N. & MacVicar, B.A. Ischemia opens neuronal gap junction hemichannels. *Science* **312**, 924–927 (2006).

ONLINE METHODS

All experiments were carried out in compliance with the relevant laws and guidelines set by the Canadian Council for Animal Care and with the approval of the University Health Network Animal Care Committee.

Expression constructs. An siRNA sequence targeted to TRPM7, corresponding to coding regions 5,152–5,172 relative to the first nucleotide of the start codon of murine TRPM7 (AAG AGT GCA TGA CTG GTG AAT, GenBank accession number AY032951)[9], or a mismatch negative control siRNA sequence (ACT ACC GTT GTA TAG GTG) was inserted into the pSilencer 3.0-H1 expression vector (Ambion). The H1 promoter-sense-loop-antisense-termination region was excised and subcloned into the pAdTrack adeno-associated viral shuttle vector to produce a vector having EGFP driven by a separate CMV promoter. We previously studied this 21-bp siRNA sequence, but only as delivered using a conventional siRNA transfection reagent or as an shRNA packaged in an adenoviral vector. These approaches suppressed TRPM7 mRNA and activity in both cortical[9] and hippocampal cultures[20], but adenoviral vectors only infected a small proportion of exposed neurons. Here, we used the same vector, but packaged in an AAV vector. Further details are provided in the **Supplementary Notes**.

AAVs. HEK293 cells were transfected with serotype 1 adeno-associated viruses (AAV1) and helper plasmids using standard CaPO$_4$ transfection. Cells were harvested 60 h after transfection and AAV1 vectors were purified from the cell lysate by ultracentrifugation through an iodixanol density gradient followed by Q column purification, and then concentrated and dialyzed using phosphate-buffered saline (PBS). Vectors were titered using real-time PCR (ABI Prism 7700) and all vector stocks diluted to 3.8×10^{12} genomes per ml[43]. Further details are provided in the **Supplementary Notes**.

Viral vector administration *in vivo*. Under ketamine/xylazine anesthesia (100 mg and 50 mg per kg of body weight, respectively), we made a midline skin incision between the bregma and interaural line. The stereotaxic coordinates for the hippocampus were 3.3 mm posterior to bregma (anterior-posterior), 2.0 mm lateral to the midline (medial-lateral) and 2.6 mm below the dura (dorsal-ventral)[44]. rAAV vectors (3.8×10^{12} genomes per ml) were microinjected through a 1-mm craniotomy in a volume of 2 μl of rAAV stock plus 1 μl of 20% mannitol (vol/vol; Sigma) in PBS[45] using a 10-μl Hamilton syringe with a 26 gauge needle. The infusion rate was 0.2 μl min^{-1} for 15 min and the needle stayed in place for another 10 min after the injection[45]. The needle was then slowly withdrawn and bone wax was applied to the craniotomy. Rats were allowed to recover for 7 to 14 d.

Immunohistochemistry of hippocampal sections and cell cultures. Immunostaining was performed as described previously[46]. In brief, hippocampal sections were blocked using 3% normal goat or rabbit serum (vol/vol), 0.3% Triton X-100 (vol/vol) and 1% BSA (vol/vol) in PBS at 20–22 °C for 90 min. Neuronal cell cultures on coverslips treated with rAAV$_{EGFP}$, rAAV$_{shSCR}$ and rAAV$_{shTRPM7}$ were fixed and cryo-protected in 2.5% sucrose (vol/vol) with 4% paraformaldehyde (wt/vol) in PBS at 20–22 °C for 20 min. The coverslips were then blocked using 1% BSA, 3% goat serum and 0.3% Triton X-100 in PBS solution for 90 min. Samples were then double or triple labeled with goat antibody to TRPM7 (#ab729, 1:50, Abcam) or rabbit antibody to TRPM2 (#ab11168, 1:50, Abcam) and mouse antibody to NeuN (#MAB377, 1:100, Chemicon) overnight at 4 °C in a rocker. NeuN is a neuron-specific marker[47]. The sections were subsequently washed in PBS and blocked briefly with the blocking solution. Subsequently, the sections were incubated with the affinity-purified second antibody, rabbit antibody to goat Alexa 568 (1:100, Molecular Probes), goat antibody to rabbit Alexa568 (1:100, Molecular Probes) and goat antibody to mouse Alexa 350 (1:100, Molecular Probes) for 1 h at 20–22 °C. Slides were finally coverslipped and mounted using ProLong Gold antifade reagent with and without DAPI (Invitrogen and Molecular Probes).

Hippocampal slice preparation for electrophysiology. Wistar rats, infected with the rAAV vectors by stereotaxic injection, were anesthetized with isoflurane and decapitated. The brains were rapidly removed and submerged in chilled (4 °C) artificial cerebrospinal fluid (aCSF) comprising 124 mM NaCl, 3 mM KCl, 2.6 mM CaCl$_2$, 1.3 mM MgCl$_2$, 26 mM NaHCO$_3$, 1.25 mM NaH$_2$PO$_4$ and 10 mM glucose (300–310 mOsmol, pH 7.4). Both hippocampi were isolated, mounted

on a block of agar and sliced (300–400 μm) using a vibratome (VT1000E, Leica). After at least 1 h in a submerged holding chamber at 20–22 °C, they were transferred to a recording chamber on an Olympus BX51WI microscope equipped with differential interference contrast and epifluorescence optics and were continuously superfused with aCSF at a rate of 3 ml min^{-1}. EGFP fluorescence, a marker of successful infection by rAAV vectors, was confirmed in all slices before recording. Field recordings were conducted at 31 ± 2 °C and whole-cell voltage- and current-clamp recordings were made at 20–22 °C. Further details are provided in **Supplementary Notes**.

Field recordings and LTP. Field EPSPs (fEPSPs) were evoked every 20 s (0.05 Hz) by electrical stimulation (100-μs duration) delivered to the Schaffer-collateral pathway using a concentric bipolar stimulating electrode (25-μm exposed tip) and recorded using glass microelectrodes (3–5 MΩ, filled with aCSF) positioned in the stratum radiatum of the CA1 area. The input-output relationship was determined in each slice by varying the stimulus intensity (100–1,000 μA) and recording the corresponding fEPSP. Using a stimulus intensity that evoked a 30–40% of maximum fEPSP, paired-pulse responses were recorded by delivering two electrical stimuli in rapid succession at intervals (interpulse interval) ranging from 10–1,000 ms. Following this assessment, the stability of synaptic responses, evoked using the same stimulus intensity as used for the paired-pulse protocol, was monitored for 20 min, at which time LTP was induced by three 1-s, 100-Hz trains of stimuli delivered 20 s apart. All field data are expressed as mean ± s.e.m. Statistical difference between means was determined by ANOVA. Further details are provided in the **Supplementary Notes**.

Recordings from acutely isolated hippocampal neurons. The preparation of acutely isolated neurons were performed as previously described[48]. Briefly, Wistar rats, infected by stereotaxic injection at 3 weeks of age with the rAAV vectors as described, were anesthetized with halothane and decapitated at 4–5 weeks of age. Hippocampi were rapidly removed and placed in cold, oxygenated ECS, cut with a razor blade into 0.5–1 mm slices and allowed to recover at 20–22 °C for 45 min. Slices were digested for 30 min at 20–22 °C in ECS containing 2.5 mg ml^{-1} papaya latex (Sigma) and then maintained, until needed, in oxygenated ECS for periods of up to 8–10 h. GFP fluorescence, a marker of successful infection by rAAV vectors, was confirmed in all slices before recording. Hippocampal CA1 pyramidal neurons were isolated from the CA1 region using fine forceps to mechanically abrade the CA1 region of GFP-positive slices. Details of the tight-seal whole-cell recordings are provided in the **Supplementary Notes**.

Global cerebral ischemia (4VO). Male Wistar rats (250–300 g, Charles River) underwent hippocampal microinjections of rAAV vectors 7 d prior. On the day of ischemia, they were anesthetized with isoflurane (3% induction and 1–1.5% maintenance, mixed with oxygen) and breathed spontaneously. Body temperature was controlled and maintained at 37 ± 0.5 °C by a heating lamp. A 15-min transient global ischemia was induced by 4VO (occluding both common carotid arteries and vertebral arteries)[27]. During the carotid artery ligation, the following parameters were assessed to assure the successful occlusion: completely flat bi-temporal electroencephalogram, dilated pupils, absence of corneal reflex and steady body temperature readings. Rats were allowed to recover for 3, 7 or 30 d before any further immunohistochemistry, histological, functional or behavioral evaluations.

Contextual fear memory. Fear conditioning was performed as previously described[49]. In brief, the conditioning chamber consisted of a Perspex arena with a light mounted in the lid (350 × 200 × 193 mm, Technical and Scientific Equipment). The floor consisted of stainless steel bars (4 mm in diameter, 5 mm apart) that were connected to a computer, which controlled the duration, timing and intensity of the shock. On day 1, single subjects were allowed to explore the chamber for 180 s. They then received three unsignaled foot shocks (2-s duration, 0.7-mA intensity) at 60-s intervals. On day 2, 24 h after the conditioning session, the rats were returned to the same chamber and the freezing response was assessed immediately and then every 8 s for 8 min. The freezing response was defined as the lack of any movement except that required for breathing. The contextual fear conditioning scores were analyzed with a one-way ANOVA, and *post hoc* analysis consisted of the Tukey-Kramer method for unequal sample sizes with the *P* value set at 0.05.

MWM. The MWM consisted of a circular pool (2.0 m in diameter, 0.8 m high) constructed of white fiberglass. The water was maintained at 22 ± 2 °C and was made opaque by the addition of a white nontoxic paint. During testing in the water maze, a platform (15 cm in diameter) was located 1.5 cm below the water surface in one of four quadrant locations, approximately 35 cm from the sidewalls. The pool was surrounded by many external extra-maze cues. A video camera was mounted in the ceiling above the pool and was connected to a video-recorder and tracking device (HVS 2020 water maze software), which permitted on- and off-line automated tracking of the path taken by the rats. The rats were subjected to four learning acquisition trials per session 7 d after a 15-min 4VO insult for five consecutive days (7–11 d post-ischemia), during which they were trained to locate the hidden escape platform, which remained in a fixed location throughout the testing. Trials lasted a maximum of 60 s and if a rat failed to find the platform in this time frame, it was gently guided to the platform by the experimenter. The rats were allowed to remain on the platform for 10 s to increase the difficulty of the task, with a 1-min rest period between trials. The rats were then tested in a probe trial 4 h after the final session on day 5 (11 d post-ischemia). For the probe trial, the platform was removed from the pool and the rat was released from the quadrant opposite where the platform had been initially located. The length of the probe trial was 60 s, after which the rat was taken out of the pool. The proportion of time the rat spent searching for the platform in the training quadrant, that is, the previous location of the platform, was recorded and used as a measure of spatial memory retention. Swim speed was also recorded to determine whether differences in motivation or motor impairment were caused by 4VO or the rAAV injection. Multivariate analysis of variance with one level repeated (day of testing)

and one level not repeated (treatment) was used to analyze the acquisition and the swim speed data over the days of training. The probe trial data were analyzed using a two-way ANOVA, and *post hoc* analysis consisted of the Tukey-Kramer method with the *P* set at 0.05.

Statistics. Data are presented as mean ± s.e.m. Unless otherwise indicated, group data were compared using one-way ANOVA and the Fisher LSD test (SigmaStat 3.0, SPSS). All experiments and analyses were performed by observers blinded to the treatment groups.

43. Lawlor, P.A. *et al.* Novel rat Alzheimer's disease models based on AAV-mediated gene transfer to selectively increase hippocampal Aβ levels. *Mol. Neurodegener.* **2**, 11 (2007).
44. Paxinos, G. & Watson, C. *The Rat Brain in Stereotaxic Coordinates* (Academic Press, San Diego, 1998).
45. Mastakov, M.Y., Baer, K., Xu, R., Fitzsimons, H. & During, M.J. Combined injection of rAAV with mannitol enhances gene expression in the rat brain. *Mol. Ther.* **3**, 225–232 (2001).
46. Sun, H.S., Feng, Z.P., Miki, T., Seino, S. & French, R.J. Enhanced neuronal damage after ischemic insults in mice lacking Kir6.2-containing ATP-sensitive K⁺ channels. *J. Neurophysiol.* **95**, 2590–2601 (2006).
47. Mullen, R.J., Buck, C.R. & Smith, A.M. NeuN, a neuronal specific nuclear protein in vertebrates. *Development* **116**, 201–211 (1992).
48. Wang, L.Y. & MacDonald, J.F. Modulation by magnesium of the affinity of NMDA receptors for glycine in murine hippocampal neurones. *J. Physiol. (Lond.)* **486**, 83–95 (1995).
49. Cheng, V.Y. *et al.* α5GABA$_A$ receptors mediate the amnestic, but not sedative-hypnotic, effects of the general anesthetic etomidate. *J. Neurosci.* **26**, 3713–3720 (2006).